Analytic Energy Consumption of Single-Source Vehicles

In comparison with Quasi-Static Simulation (QSS), FACE is developed to fast approximate energy consumption and to optimize dimensioning parameters of a vehicle propulsion system. Based on reference vehicles and specific missions, FACE analytically approximates the energy consumption of single-source vehicles, including conventional and battery-electric vehicles. Sensitivity of powertrain dimensioning parameters is presented in simplified expressions for the intuition purpose. The FACE is further compared with QSS in terms of the energy consumption.

5.1 Conventional Vehicle

FACE, standing for Fully-Analytic energy Consumption Estimation, analytically approximates the energy consumption of a conventional vehicle with dimension-related parameters and cycle-related parameters. Dimension-related parameters consist of dimensioning parameters of powertrain components and vehicles. The dimension-related parameters are vehicle-dependent, such as engine displacement and vehicle mass. Cycle-related parameters are in function of mission variables, such as velocity and acceleration. For conventional vehicles, gear sequence is also a mission variable. For example, a cycle-related parameter can be $v^2 a n_t$. Details of the dimension- and cycle-related parameters are found in the following section.

Considering the evaluation of energy consumption, the dimension-related parameters are originated from the investigated conventional vehicle; whereas cycle-related

parameters are determined a priori based on a reference vehicle. Moreover, cycle-related parameters are influenced by the status of the internal combustion engine. Specifically, an engine converts burned fuel to mechanical power in propulsion phase; whereas the engine does not consume any fuel during the braking condition. Moreover, the idling fuel consumption is assumed to omit due to the adoption of stop-start systems.

5.1.1 Fully Analytic Energy Consumption Estimation

Due to high performance of an internal combustion engine, the operating points over a standardized mission are often concentrated at low speed and low- and mid-load area in its efficiency map. Thus, only the first case of the light-duty engine piece-wise model is implemented in FACE. Combining analytic models of internal combustion engine in Eq. 2.2 (only first case), transmission in Eq. 2.24 and 2.25, and vehicle load model in Eq. 2.38, the power of burned fuel at time t is written by

$$P_{ef} = k_{e0} + \frac{k_{e1} C_{v0} v}{k_{t5}} + \frac{k_{e1} C_{v1} v^2 + k_{e1} C_{v2} v^3 + k_{e1} v a}{k_{t5}}, \tag{5.1}$$

where P_{ef} is valid only when vehicle load $F_l > 0$.

Descriptive parameters in Eq. 5.1, such as k_{e0}, k_{e1}, and k_{t5}, are substituted with their corresponding predictive models introduced in Chapter 2. Thus, dimensioning parameters constitute the dimension-related parameters, which depend on the investigated vehicle. Then, cycle-related parameters are separated in each term of the full expansion of Eq. 5.1. Because of the implementation of a reference vehicle, cycle-related parameters are constant in FACE.

Consisting of dimension-related variables and cycle-related parameters, FACE for conventional vehicles is expressed as

$$E_{ef} = \sum_{i=1,j=0,k=0}^{i=5,j=1,k=8} \mathcal{D}_{ijk} \mathcal{C}_{ijk}, \tag{5.2}$$

where $\mathcal{D}_{ijk}$ are dimension-related variables of the investigated vehicle, and $\mathcal{C}_{ijk}$ are cycle-related parameters of a reference vehicle, subscripts i, j, k correspond to the exponents of velocity, acceleration, and gear number.

The dimension of the full expansion of Eq. 5.2 is so large that both dimension-and cycle-related parameters are simplified. Details of each dimension-related parameter are found in Appendix D.1. As for the cycle-related parameters based on a reference

vehicle, they are summarized by

$$\mathcal{C}_{ijk} = \sum_{t \in \sigma} v^i(t) a^j(t) n_t^k(t) \Delta t, \tag{5.3}$$

where the mission variables – including, velocity v, acceleration a, and gear shift schedule n_t – the set of effective time steps σ, and the time interval Δt are involved.

The set of effective time steps σ is defined by

$$\sigma = \left\{ t : F_l(t) > 0, t \in [t_0,\ t_f] \right\}, \tag{5.4}$$

where F_l is vehicle load estimated in Eq. 2.38, σ is the set of valid time steps based on the reference vehicle.

Since not all of the combinations of i, j, and k exist in FACE, the valid combinations for conventional vehicles are summarized as

$$\begin{aligned}
&i = 1, jk = \{00, 01, 02, 03, 04, 10\}, \\
&i = 2, jk = \{00, 01, 02, 03, 04, 05, 06, 07, 08, 10, 11, 12, 13, 14\}, \\
&i = 3, jk = \{00, 01, 02, 03, 04, 05, 06, 07, 08, 10, 11, 12, 13, 14, 15, 16, 17, 18\}, \\
&i = 4, jk = \{00, 01, 02, 03, 04, 05, 06, 07, 08\}, \\
&i = 5, jk = \{00, 01, 02, 03, 04, 05, 06, 07, 08\}.
\end{aligned} \tag{5.5}$$

5.1.2 Sensitivity of Dimensioning Parameters

Although FACE is developed, relations between energy consumption and powertrain dimensioning parameters are implicit in Eq. 5.2. To make FACE more intuitive, sensitivity of powertrain dimensioning parameters proffers explicit relations below.

Concerning dimensioning parameters of internal combustion engines, the energy consumption is a linear function of engine displacement, which yields

$$E_{ef}(\mathcal{V}_e) = \kappa_{e0} + \kappa_{e1} \mathcal{V}_e, \tag{5.6}$$

where parameters $\kappa_{(\dots)}$ are generic and derived from Eq. 5.2. Expressions of parameters κ will not be fully expanded for simplicity reason.

Regarding the dimensioning parameters of drivetrain, quadratic models are feasible to the gear ratios of first and last gear ($\mathcal{R}_{t1}$ and $\mathcal{R}_{tk}$) and the ratio of final drive ($\mathcal{R}_{fd}$),

which are given by

$$E_{ef}(\mathcal{R}_{t1}) = \kappa_{t0} + \kappa_{t1}\mathcal{R}_{t1} + \kappa_{t2}\mathcal{R}_{t1}^2, \tag{5.7}$$

$$E_{ef}(\mathcal{R}_{tk}) = \kappa_{t3} + \kappa_{t4}\mathcal{R}_{tk} + \kappa_{t2}\mathcal{R}_{tk}^2, \tag{5.8}$$

$$E_{ef}(\mathcal{R}_{fd}) = \kappa_{d0} + \kappa_{d1}\mathcal{R}_{fd} + \kappa_{d2}\mathcal{R}_{fd}^2. \tag{5.9}$$

Note that, the overall gear ratios are considered for $\mathcal{R}_{t1}$ and $\mathcal{R}_{tk}$ if the final drive is of multiple speeds. Meanwhile, the ratio $\mathcal{R}_{fd}$ is assumed to be one in this condition.

In addition, energy consumption is also expressed as functions of vehicle parameters. Since parameter C_{v0} is approximated by $C_{v0} \approx m_v g C_{rr}$, the relations between the energy consumption and vehicle parameters are separately presented as

$$E_{ef}(C_{v2}) = \kappa_{v0} + \kappa_{v1}C_{v2}, \tag{5.10}$$

$$E_{ef}(C_{v1}) = \kappa_{v2} + \kappa_{v3}C_{v1}, \tag{5.11}$$

$$E_{ef}(C_{v0}) = \kappa_{v4} + \kappa_{v5}C_{v0}, \tag{5.12}$$

$$E_{ef}(m_v) = \kappa_{v6} + \kappa_{v7}m_v. \tag{5.13}$$

5.2 Battery-Electric Vehicle

To optimize the dimensioning parameters of powertrain components, FACE is also developed for battery-electric vehicles with single-speed transmissions. Similar to conventional vehicles, FACE estimates the energy consumption of a battery-electric vehicle with dimension- and cycle-related parameters. Dimension-related parameters associate with a battery-electric vehicle to investigate, including battery, electric motor/generator, and single-speed transmission; whereas cycle-related parameters are mission-dependent and reference-vehicle-dependent constants.

In a battery-electric vehicle, battery is discharged as an energy source to propel the vehicle. Yet, it can also be charged to recuperate energy during braking. These operations segment the analytic model of battery electrochemical power into to conditions because of the efficiency of the drivetrain. The standstill operation is included in the propelling operation.

5.2.1 Fully Analytic Energy Consumption Estimation

The consumed electrochemical power of battery is calculated in a piecewise function by combining analytic models of battery in Eq. 2.30 (the quadratic model), electric motor/generator in Eq. 2.35, and single-speed transmission in Eq. 2.22 and 2.25, and vehicle load model in Eq. 2.38.

In the fully expanded electrochemical power of battery, the same items of mission variables are merged that account for the cycle-related parameters. The rest terms, consisting of powertrain dimensioning parameters and constants, make up the dimension-related parameters.

Because of its too large dimension, the expression of FACE for battery-electric vehicles is simplified as

$$E_{be} = \sum_{\beta=1}^{2} \sum_{i=0,j=0}^{i=8,j=4} \mathcal{D}_{ij}^{b\beta} \mathcal{C}_{ij}^{\beta}, \ (\beta = 1, 2), \tag{5.14}$$

where β refers traction ($\beta = 1$) and braking operation ($\beta = 2$); $\mathcal{D}_{ij}^{b\beta}$ are dimension-related parameters in accordance with vehicle operating conditions; and $\mathcal{C}_{ij}^{\beta}$ are cycle-related parameters based on a reference vehicle.

The detailed dimension-related parameters are listed in Appendix D.2; whereas the cycle-related parameters of a reference battery-electric vehicle are summarized as

$$\mathcal{C}_{ij}^{\beta} = \sum_{t \in \sigma_{b\beta}} v^i(t) a^j(t) \Delta t, \ (\beta = 1, 2), \tag{5.15}$$

where $\sigma_{b\beta}$ are sets of time steps corresponding to vehicle operating conditions.

The time sets $\sigma_{b\beta}(\beta = 1, 2)$ in accordance with the operating conditions of a reference vehicle are summarized in an overall time set $\sigma_{b\beta}$, which yields

$$\sigma_{b\beta} = \begin{Bmatrix} \sigma_{b1} = \{t : F_l(t) \geq 0\} \\ \sigma_{b2} = \{t : F_l(t) < 0\} \end{Bmatrix}. \tag{5.16}$$

The existing combinations of i and j in Eq. 5.14 and 5.15 are summarized as

$$\begin{aligned} i &= \{0, 1, 2, 3, 4, 5, 6, 7, 8\}, \ j = 0, \\ i &= \{0, 1, 2, 3, 4, 5, 6\}, \ j = 1, \\ i &= \{0, 1, 2, 3, 4\}, \ j = 2, \end{aligned} \tag{5.17}$$

$$i = \{0, 1, 2\},\ j = 3,$$
$$i = \{0\},\ j = 4.$$

Because of the implemented transmissions, the FACE in this section is dedicated to battery-electric vehicles of single-speed transmissions.

5.2.2 Sensitivity of Dimensioning Parameters

Explicit relations between energy consumption and powertrain dimensioning parameters (including vehicle parameters) are formulated to make FACE intuitive and obvious.

Concerning dimensioning parameters of battery, FACE is nonlinear as a function of battery cell number $\mathcal{K}_b$ and battery cell capacity $\mathcal{Q}_b$ as expressed by

$$E_{be}(\mathcal{K}_b) = \kappa_{b0} + \kappa_{b1}\mathcal{K}_b + \frac{\kappa_{b2}}{\mathcal{K}_b}, \tag{5.18}$$
$$E_{be}(\mathcal{Q}_b) = \kappa_{b3} + \kappa_{b4}\mathcal{Q}_b + \kappa_{b5}\mathcal{Q}_b^2. \tag{5.19}$$

Regarding to dimensioning parameters of electric motor/generators, FACE is a fourth degree polynomial as a function of rated torque $\mathcal{T}_m$ and of base speed $\mathcal{N}_m$. The quartic polynomials are re-written by

$$E_{be}(\mathcal{T}_m) = \kappa_{m0} + \kappa_{m1}\mathcal{T}_m + \kappa_{m2}\mathcal{T}_m^2 + \kappa_{m3}\mathcal{T}_m^3 + \kappa_{m4}\mathcal{T}_m^4, \tag{5.20}$$
$$E_{be}(\mathcal{N}_m) = \kappa_{m5} + \kappa_{m6}\mathcal{N}_m + \kappa_{m7}\mathcal{N}_m^2 + \kappa_{m8}\mathcal{N}_m^3 + \kappa_{m9}\mathcal{N}_m^4. \tag{5.21}$$

With regard to dimensioning parameters of a drivetrain, high nonlinearity of FACE exists, such as

$$E_{be}(\mathcal{R}_t) = \sum_{i=0}^{4} \kappa_{di}\mathcal{R}_t^i + \frac{\kappa_{d5}}{\mathcal{R}_t} + \frac{\kappa_{d6}}{\mathcal{R}_t^2} + \frac{\kappa_{d7}}{\mathcal{R}_t^4}, \tag{5.22}$$
$$E_{be}(\mathcal{R}_{fd}) = \sum_{i=0}^{4} \kappa_{di}\mathcal{R}_{fd}^i + \frac{\kappa_{d5}}{\mathcal{R}_{fd}} + \frac{\kappa_{d6}}{\mathcal{R}_{fd}^2} + \frac{\kappa_{d7}}{\mathcal{R}_{fd}^4}. \tag{5.23}$$

Relations between energy consumption and vehicle parameters are given by

$$E_{be}(C_{v2}) = \kappa_{v0} + \kappa_{v1}C_{v2} + \kappa_{v2}C_{v2}^2 + \kappa_{v3}C_{v2}^3 + \kappa_{v4}C_{v2}^4, \tag{5.24}$$
$$E_{be}(C_{v1}) = \kappa_{v5} + \kappa_{v6}C_{v1} + \kappa_{v7}C_{v1}^2 + \kappa_{v8}C_{v1}^3 + \kappa_{v9}C_{v1}^4, \tag{5.25}$$

$$E_{be}(C_{v0}) = \kappa_{v10} + \kappa_{v11}C_{v0} + \kappa_{v12}C_{v0}^2 + \kappa_{v13}C_{v0}^3 + \kappa_{v14}C_{v0}^4, \tag{5.26}$$

$$E_{be}(m_v) = \kappa_{v15} + \kappa_{v16}m_v + \kappa_{v17}m_v^2 + \kappa_{v18}m_v^3 + \kappa_{v19}m_v^4. \tag{5.27}$$

5.3 Analytic Evaluation of Energy Consumption

FACE is applied to approximate the energy consumption of several single-source vehicles. The energy consumption is compared based on the evaluation with different methods, such as of FACE and Quasi-Static Simulations (QSS). The predictive analytic models of powertrain components are applied to the evaluation of energy consumption through FACE. Instead, the grid-point data is used in the evaluation via QSS. As a result, errors of different types of powertrain data is introduced.

5.3.1 Conventional Vehicle

Conventional vehicles of different engine technologies but same drivetrain and vehicle are investigated through both FACE and QSS. Note that, the type of powertrain models in FACE is different from that in QSS.

Reference Vehicles

Main characteristics of the investigated conventional vehicles are summarized in Table 5.1. The reference vehicle (Vehicle I) and the investigated vehicles (Vehicle II, III, and IV) have the same vehicle parameters and drivetrain. The varied dimension-related variables are composed of engine displacement and the engine rated torque and power. In addition, Vehicle I is used to estimate the cycle-related parameters for the evaluation of fuel consumption of Vehicle II, III, and IV over various missions.

Results and Analysis

Comparisons of fuel consumption are illustrated in Fig. 5.1. The highest error between FACE and QSS is presented by Vehicle I over FTP-72, which is 3.85%. As for the least one, it is about 0.83% of Vehicle II over HYWFET. However, there are several sources of errors that could impact the comparisons. Firstly, models of powertrain components are different, which are grid-point data and predictive analytic model. Secondly, FACE is developed based on the first case of light-duty engine model in Eq. 2.2, which means engine power that is larger than the corner power ($P_e > P_{ec}$) requires

Vehicle		I	II	III	IV
	m_v [kg]	1595			
	R_w [m]	0.3017			
	C_{v0} [N]	134.094			
	C_{v1} [N/(m/s)]	3.747			
	C_{v2} [N/(m/s)^2]	0.3486			
Engine	$\mathcal{I}_e$	CI/TC	SI/TC	SI/NA/LB	SI/NA/SB
	$\mathcal{V}_e$ [L]	2.1	2.1	1.9	1.9
	$\mathcal{T}_e$ [Nm]	292	302	166	166
	$\mathcal{P}_e$ [kW]	90	150	80	80
Drivetrain	$\mathcal{I}_t$	DCT-6			
	$\mathcal{R}_{fd}$	4.12 & 3.04			

Table 5.1 – Main features of investigated conventional vehicles.

less fuel consumption. The reference cycle-related parameters may affect the energy consumption as well. In addition, accumulative effect is not negligible due to repeated or very similar operating points.

Taking the errors between models of powertrain components into account, good accuracy allows FACE to approximate fuel consumption and to optimize powertrain dimensioning parameters.

5.3.2 Battery-Electric Vehicle

Two battery-electric vehicles with different electric motor/generators are investigated to show the accuracy of FACE.

Reference Vehicles

Features of the investigated battery-electric vehicles are listed in 5.2, in which Vehicle I is the reference vehicle for the evaluation of cycle-related parameters.The dimension-related variables are composed of the rated torque and power of electric motors.

The battery-electric vehicles are investigated through QSS and FACE over three missions. The energy consumption is depicted in Fig. 5.2. Considering the powertrain model of the electric motor/generators, grid-point data is implemented in the evaluation of QSS; whereas predictive analytic models are applied in the approximation of FACE.

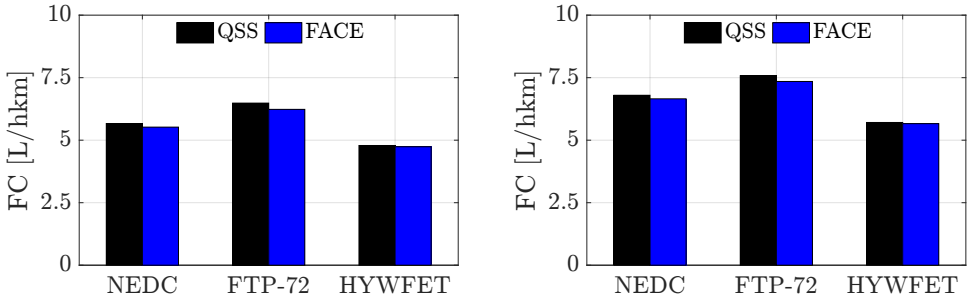

(a) Vehicle I

(b) Vehicle II

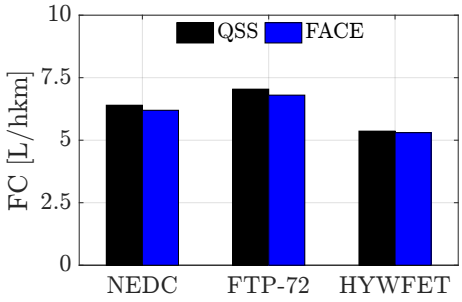

(c) Vehicle III

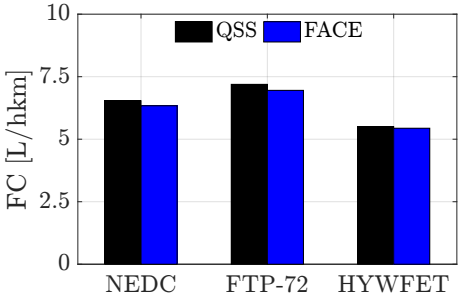

(d) Vehicle IV

Figure 5.1 – Fuel consumption of conventional vehicles evaluated through QSS and FACE.

Vehicle		I	II
	m_v [kg]	1648	
	R_w [m]	0.3952	
	C_{v0} [N]	141.947	
	C_{v1} [N/(m/s)]	1.153	
	C_{v2} [N/(m/s)^2]	0.3952	
Battery	$\mathcal{I}_b$	HE	
	$\mathcal{Q}_b$ [Ah]	31	
	$\mathcal{K}_b$	192	
Electric Motor	$\mathcal{I}_m$	PMSM	
	$\mathcal{T}_m$ [Nm]	108	108
	$\mathcal{P}_m$ [kW]	79	45
Drivetrain	$\mathcal{R}_d$	14	

Table 5.2 – Main features of investigated battery-electric vehicles.

Results and Analysis

Results of energy consumption of the reference and investigated vehicles are shown in Fig. 5.2, where Vehicle I is the reference. The energy consumption of Vehicle I is evaluated via the fully analytic approach, in which the cycle-related parameters do not cause any error. The greatest error of 7.69% is found, which is mainly caused by the model errors between grid-point data and the predictive analytic models of the electric motor/generator.

However, the differences of energy consumption of Vehicle II are smaller than Vehicle I over all investigated missions. FACE universally underestimates the energy consumption. The errors are caused by powertrain models, reference vehicle, and cumulation of similar operations of the electric motor/generator. Nonetheless, Vehicle II shows a good approximation (see Fig. 5.2b).

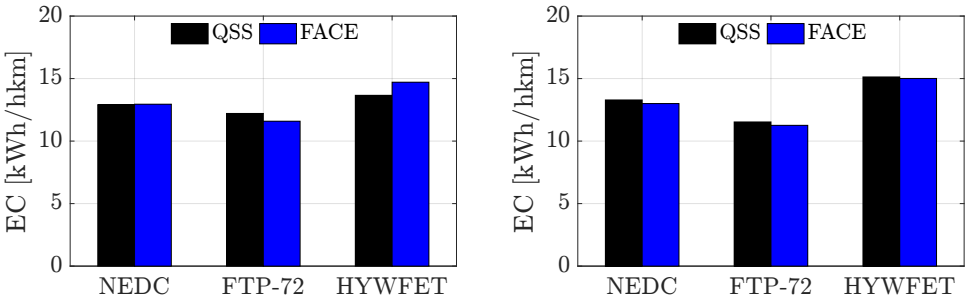

(a) Vehicle I (b) Vehicle II

Figure 5.2 – Energy consumption of battery-electric vehicles evaluated with QSS and FACE

Chapter 6

Analytic Minimal Energy Consumption of Hybrid-Electric Vehicles

Compared with single-source vehicles, the mandatory control optimization for the evaluation of the minimal energy consumption significantly augments the complexity of the development of Fully-Analytic energy Consumption Estimation (FACE) for hybrid-electric vehicles. Nevertheless, FACE is developed based on distinct ideas for series and parallel hybrid-electric vehicles.

6.1 Series Hybrid-Electric Vehicle

For series hybrid-electric vehicles, FACE approximates the minimal energy consumption based on further simplified GRAB-ECO. The simplification requires an analytic model of an Auxiliary Power Unit (APU).

6.1.1 Auxiliary Power Unit

The operating point of an APU owning the best efficiency is analytically modeled by

$$\eta^*_{apu} = -\frac{128k_{g0}\pi^9}{\mathbf{p}_3\mathcal{V}_e\omega_{ei}} - \frac{128k_{g1}\pi^9\mathcal{R}_g}{\mathbf{p}_3\mathcal{V}_e} - \frac{128k_{g2}\pi^9\mathcal{R}_g^2\omega_{ei}}{\mathbf{p}_3\mathcal{V}_e} + \frac{125k_{g3}\mathbf{p}_2}{\mathbf{p}_3\omega_{ei}} - \frac{15625k_{g4}\mathbf{p}_1^2\mathcal{V}_e}{128\pi^9\mathcal{R}_g^2\mathbf{p}_3\omega_{ei}} + \frac{\mathbf{n}_1}{\mathbf{d}_1} + \frac{\mathbf{n}_2}{\mathbf{d}_2}, \tag{6.1}$$

where $\mathbf{n}_i(i = 1,\ 2)$ and $\mathbf{d}_i(i = 1,\ 2)$ are numerator and denominator terms, respectively; and $\mathbf{p}_i(i = 1, \cdots, 11)$ are polynomials, some of which are nested in $\mathbf{n}_i(i = 1,\ 2)$ and $\mathbf{d}_i(i = 1,\ 2)$.

Fig. 6.1 depicts the efficiency of the best-efficiency point evaluated with analytic model (denoted by η^*_{apu}), and the efficiency of the optimal operating line (indicated by η_{apu}) as a function of engine speed for different gear ratios $\mathcal{R}_g$ between the internal combustion engine and the electric generator.

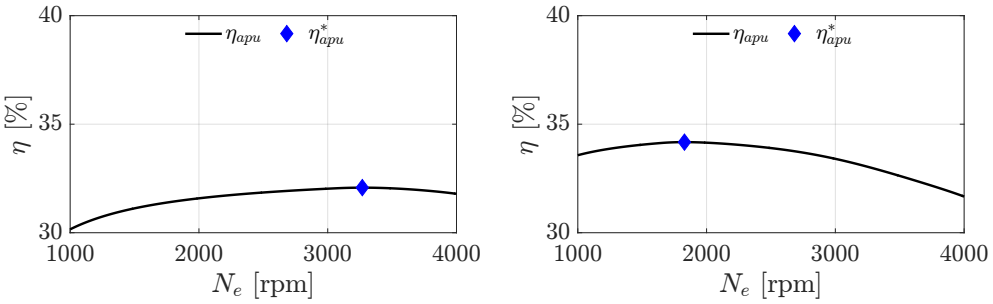

(a) $\mathcal{R}_g = 2.3$ (b) $\mathcal{R}_g = 3.5$

Figure 6.1 – Best-efficiency point of APU in terms of gear ratio.

As a supplementary, the impacts of engine displacement on the best-efficiency point of APU are illustrated in Fig. 6.2a. The developed analytic model of best-efficiency point can predict the best efficiency.

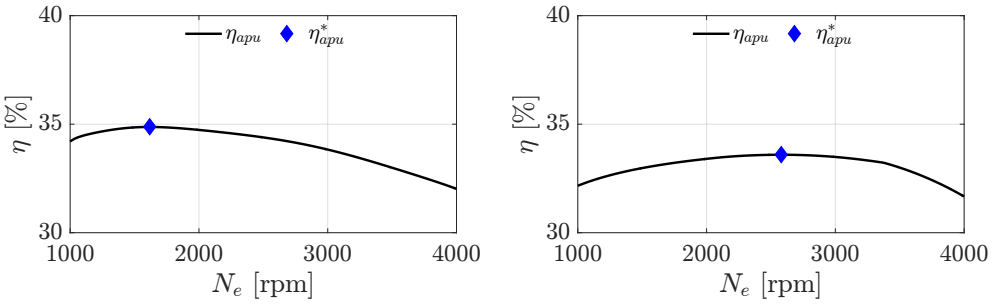

(a) $\mathcal{V}_e = 1.2$ L (b) $\mathcal{V}_e = 2.2$ L

Figure 6.2 – Best-efficiency point of APU in terms of engine displacement.

6.1.2 Fully Analytic Energy Consumption Estimation

Considering the optimal control problem of series HEVs, it is simplified based on GRAB-ECO. The idea is to assume that a series HEV drives like a battery-electric vehicle over a given mission. At the end of the mission, battery is depleted due to various external resistances and powertrain efficiencies. The depleted energy is ultimately recuperated by recharging the battery with APU that works at its best-efficiency operating point.

Based on the developed analytic model of the best-efficiency point of an APU in Eq. 6.1, FACE fully involves dimensioning parameters of internal combustion engines, electric generators, and simple gear train $\mathcal{R}_g$ for series hybrid-electric vehicles.

The FACE combines the consumed electrochemical energy of battery-electric vehicles in Eq. 5.14 and the analytic model of APU in Eq. 6.1. Therefore, FACE is expressed as

$$E_{ef} = \frac{\sum\limits_{t\in\sigma_{b\beta}} P_{be}^{\beta}(t)\Delta t}{\eta_{apu}^{*}}, \ (\beta = 1, 2), \tag{6.2}$$

where time sets $\sigma_{b\beta}(\beta = 1, 2)$ are the same as those for battery-electric vehicles.

The analytic model of best-efficiency point is independent from the cycle-related parameters. As a result, the minimal energy consumption model in Eq. 6.2 can be further simplified by lumping the analytic model in Eq. 6.1 into dimension-related variables, which yields

$$E_{ef} = \sum_{\beta=1}^{2} \sum_{i=0,j=0}^{i=8,j=4} \mathcal{D}_{ij}^{b\beta} \mathcal{C}_{ij}^{\beta}, \ (\beta = 1, 2). \tag{6.3}$$

Despite the same form as battery-electric vehicles, FACE approximates the minimal fuel energy consumption for series HEVs. The analytic model relating to APU in Eq. 6.3 is involved in the dimension-related variables $\mathcal{D}_{ij}^{b\beta}$. Concerning the cycle-related parameters in Eq. 6.3, they are exactly the same as that for battery-electric vehicle in Eq. 5.15.

6.2 Parallel Hybrid-Electric Vehicle

FACE for parallel hybrid-electric vehicles is developed based on SHM with a few essential assumptions Thus, the anticipated difficulties consist of combined analytic model of battery and electric motor/generator, estimation of the proper adjoint state variable, and an analytic model of the minimal energy approximation. Methods to resolve these

problems are individually introduced hereafter.

6.2.1 Analytic Model of Assembled Battery and Motor

In Section 4.3, Selective Hamiltonian Minimization (SHM) is developed based on the quadratic analytic model of battery in Eq. 2.30 for the sake of better accuracy, full operating range, and resulting shorter computational time. However, the analytic model of assembled battery and electric motor in Eq. 4.23 cannot directly account for dimensioning parameters of battery and electric motor/generator. Therefore, the bi-linear model of battery in Eq. 2.31, instead of the quadratic one, is implemented to encompass dimensioning parameters of battery and electric motor. Consequently, the analytic model of the combined battery and electric motor is given by

$$P_{be} = \begin{cases} k_{b3} + k_{b4}(k_{m0} + k_{m1}\omega_m + k_{m2}\omega_m^2) + k_{b4}k_{m3}P_m + \dfrac{k_{b4}k_{m4}}{\omega_m^2}P_m^2, & P_m \geq 0, \\ k_{b5} + k_{b6}(k_{m0} + k_{m1}\omega_m + k_{m2}\omega_m^2) + k_{b6}k_{m3}P_m + \dfrac{k_{b6}k_{m4}}{\omega_m^2}P_m^2, & P_m < 0. \end{cases} \tag{6.4}$$

As a result, the possible solutions to the optimal control problem in Eq. 4.38 is rewritten by

$$u(t,s) \in \begin{Bmatrix} P_{m,unc1}(t,s) \\ P_{m,unc2}(t,s) \\ P_d(t) \\ P_d(t) - P_{ec}(t) \\ \overline{P}_m(t) \\ \underline{P}_m(t) \\ P_d(t) - \overline{P}_e(t) \end{Bmatrix}, \tag{6.5}$$

where $P_{m,unc1}(t,s)$ and $P_{m,unc2}(t,s)$, corresponding to two cases of the bi-linear model of battery, are expressed by

$$P_{m,unc1}(t,s) = \frac{(k_{e1}(t) - sk_{b4}k_{m3})\,\omega_m^2(t)}{2sk_{b4}k_{m4}}, \tag{6.6}$$

$$P_{m,unc2}(t,s) = \frac{(k_{e1}(t) - sk_{b6}k_{m3})\,\omega_m^2(t)}{2sk_{b6}k_{m4}}. \tag{6.7}$$

Additionally, the adapted control space is further simplified by $u \in \{u_i : i = 1, \cdots, 7\}$, where subscript i indicates the i^{th} functional in the control space in Eq. 6.5.

A comparison has been made between the energy consumption based on the piece-

wise linear and the quadratic battery model. Selctive Hamiltonian Minimization (SHM) is applied to evaluate the energy consumption of a reference vehicle. As illustrated in Fig. 6.3, the bilinear model of battery has different level of errors depending on missions. The discrepancy of minimal fuel consumption is negligible over NEDC; where the differences over FTP-72 and HYWFET are slightly increased (the error is about 2.34%).

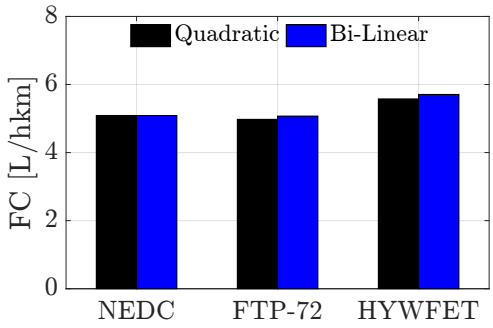

Figure 6.3 – Minimal fuel consumption of different battery models.

6.2.2 Equivalent Energy Consumption Model

To develop FACE based on SHM, an analytic model, known as the equivalent energy consumption model, is proposed to evaluate the minimal energy consumption. The equivalent energy consumption model is

$$E_{ef}^{eqv}(s) = \sum_{t=t_0}^{t_f} \Big(P_{ef}^{*}(t) + sP_{be}^{*}(t) \Big) \Delta t, \tag{6.8}$$

where E_{ef}^{eqv} is the equivalent fuel energy consumption, s is the adjoint state variable, P_{ef}^{*} is the burned fuel power resulting from optimal control laws, and P_{be}^{*} is the electrochemical power of battery based on optimal control laws.

The minimal energy consumption and the equivalent energy consumption are compared for an exemplified parallel hybrid-electric vehicle, as illustrated in Fig. 6.4. The energy of battery E_{be}, of burned fuel E_{ef}, and of equivalent energy consumption E_{ef}^{eqv} are presented as a function of adjoint state variable s. The minimal energy consumption is indicated by a red dot crossed by a horizontal red dashed line, which is determined by the proper adjoint state variable of the reference vehicle s^{ref}.

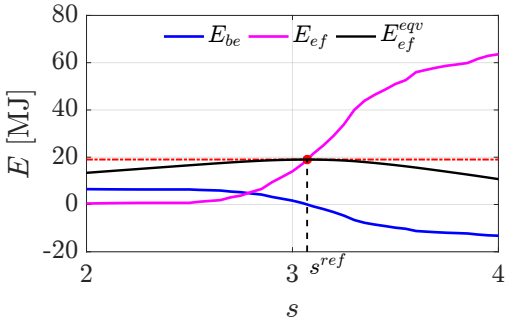

Figure 6.4 – Equivalent minimal fuel consumption of hybrid-electric vehicles.

As observed in Fig. 6.4, the minimal energy consumption is assumed to be approximated by the equivalent energy consumption for any given adjoint variable s, which yields

$$E_{ef} \approx E_{ef}^{eqv}(s),\ \forall s. \tag{6.9}$$

The equivalent energy consumption can approximate the minimal energy consumption for a hybrid-electric vehicle when the adjoint state variable s_{ref} is chosen. To further precise the approximation of equivalent fuel consumption, the adjoint state variable of a reference vehicle is used, thereby leading to

$$E_{ef} = E_{ef}^{eqv}(s^{ref}). \tag{6.10}$$

6.2.3 Fully Analytic Energy Consumption Estimation

Based on the equivalent energy consumption model and a reference hybrid-electric vehicle, the Fully Analytic fuel Energy Consumption Estimation (FACE) is expressed by

$$E_{ef} = \sum_{i,j,\epsilon,\nu} \mathcal{D}_{ij}^{e\epsilon\nu}\mathcal{C}_{ij}^{\epsilon\nu} + s^{ref}\sum_{i,j,\epsilon,\nu} \mathcal{D}_{ij}^{b\beta\nu}\mathcal{C}_{ij}^{\epsilon\nu}, \tag{6.11}$$

where $\mathcal{D}_{ij}^{e\epsilon\nu}$ and $\mathcal{D}_{ij}^{b\epsilon\nu}$ are dimension-related parameters relating to engine and battery, respectively; $\mathcal{C}_{ij}^{\epsilon\nu}$ denotes cycle-related parameters derived from a reference hybrid-electric vehicle, parameters $i, j, \epsilon,$ and ν are given by $i = 0,\cdots,6;\ j = 0,\cdots,2;\ \epsilon = 1,\cdots,10;\ \nu = 1,\cdots,\mathcal{K}_t$; and s^{ref} is the adjoint state variable of the reference vehicle.

Considering the dimension-related parameters, they are further clustered into $\mathcal{K}_t$ groups due to the stepped-ratio transmission. The dimension-related parameters are given in Appendix E.2 because of too many equations. The cycle-related parameters are summarized as

$$\mathcal{C}_{ij}^{\epsilon\nu} = \sum_{t\in\sigma_{\epsilon\nu}} v^i(t)a^j(t)\Delta t, \tag{6.12}$$

where the time set $\sigma_{\epsilon\nu}$ is defined by

$$\sigma_{\epsilon\nu} = \left\{\{t\} : u^*(t, s^{ref}) = u_\epsilon(t, s^{ref}),\ \mathcal{K}_t(t) = \nu\right\}. \tag{6.13}$$

The valid combinations of i and j for hybrid-electric vehicles are summarized as

$$\begin{aligned} i = \{0,1,2,3,4,5,6\},\ j = 0,\\ i = \{0,1,2,3\},\ j = 1,\\ i = \{0\},\ j = 2. \end{aligned} \tag{6.14}$$

A possible optimal control solution is exemplified to show how dimension- and cycle-related parameters are derived. The burned fuel power in the first unconstrained condition ($\epsilon = 1$) is expressed by

$$P_{ef}^{1\nu} = \mathcal{D}_{10}^{e1\nu}v + \mathcal{D}_{20}^{e1\nu}v^2 + \mathcal{D}_{30}^{e1\nu}v^3 + \mathcal{D}_{40}^{e1\nu}v^4 + \mathcal{D}_{50}^{e1\nu}v^5 + \mathcal{D}_{60}^{e1\nu}v^6 + \mathcal{D}_{11}^{e1\nu}va + \mathcal{D}_{21}^{e1\nu}v^2a. \tag{6.15}$$

Consequently, the energy of burned fuel in the unconstrained condition is evaluated by

$$\begin{aligned} E_{ef}^{1\nu} &= \sum_{\nu=1}^{\mathcal{K}_t}\Bigg(\mathcal{D}_{10}^{e1\nu}\sum_{t\in\sigma_{1\nu}} v + \mathcal{D}_{20}^{e1\nu}\sum_{t\in\sigma_{1\nu}} v^2 + \mathcal{D}_{30}^{e1\nu}\sum_{t\in\sigma_{1\nu}} v^3 + \mathcal{D}_{40}^{e1\nu}\sum_{t\in\sigma_{1\nu}} v^4\\ &\quad + \mathcal{D}_{50}^{e1\nu}\sum_{t\in\sigma_{1\nu}} v^5 + \mathcal{D}_{60}^{e1\nu}\sum_{t\in\sigma_{1\nu}} v^6 + \mathcal{D}_{11}^{e1\nu}\sum_{t\in\sigma_{1\nu}} va + \mathcal{D}_{21}^{e1\nu}\sum_{t\in\sigma_{1\nu}} v^2a\Bigg)\\ &= \sum_{\nu=1}^{\mathcal{K}_t}\sum_{i=0,j=0}^{i=6,j=1} \mathcal{D}_{ij}^{e\epsilon\nu}\mathcal{C}_{ij}^{\epsilon\nu}. \end{aligned} \tag{6.16}$$

The sensitivity of dimensioning parameters are not presented owing to the high

nonlinearity of FACE for parallel HEVs.

6.3 Analytic Evaluation of Minimal Energy Consumption

Energy consumption of hybrid-electric vehicles of series and parallel architectures is evaluated through FACE and compared the one via QSS.

6.3.1 Series Hybrid-Electric Vehicle

Reference Vehicles

A baseline series hybrid-electric vehicle and the one of partially varied dimensioning parameters are separately investigated with FACE and VHOT. Features of these two series HEVs are summarized in Table 6.1.

Vehicle		I	II
	m_v [kg]	1400	
	R_w [m]	0.36	
	C_{v0} [N]	137.74	
	C_{v1} [N/(m/s)]	0	
	C_{v2} [N/(m/s)^2]	0.432	
Engine	$\mathcal{I}_e$	CI	
	$\mathcal{V}_e$ [L]	0.7	
	$\mathcal{T}_e$ [Nm]	66	
	$\mathcal{P}_e$ [kW]	44	
Electric Generator	$\mathcal{I}_g$	PMSM	
	$\mathcal{T}_g$ [Nm]	90	
	$\mathcal{P}_g$ [kW]	49	
Battery	$\mathcal{I}_b$	HE	
	$\mathcal{E}_b$ [kWh]	7	
Electric Motor	$\mathcal{I}_m$	PMSM	
	$\mathcal{T}_m$ [Nm]	250	
	$\mathcal{P}_m$ [kW]	98	120

Table 6.1 – Main features of investigated series hybrid-electric vehicles.

Results and Analysis

The energy consumption in terms of fuel consumption are depicted for the reference and investigated vehicle in Fig. 6.5. The FACE approximates the minimal fuel consumption almost the same as the one by VHOT. The differences is mainly caused by the power losses of the electric components due to the simplified assumption for series hybrid-electric vehicles.

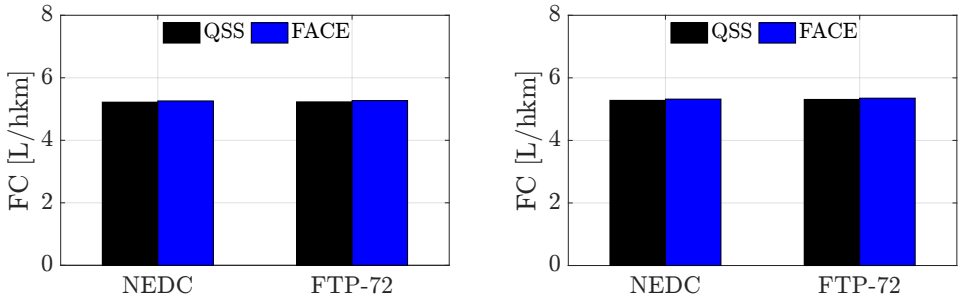

(a) Vehicle I (b) Vehicle II

Figure 6.5 – Minimal energy consumption of reference and investigated series hybrid-electric vehicles.

6.3.2 Parallel Hybrid-Electric Vehicle

Reference Vehicles

Concerning parallel hybrid-electric vehicles, the characteristics of the reference parallel HEV Vehicle I and the investigated one Vehicle II are summarized in Table 6.2. The main difference is the installed internal combustion engine. When scaling the engine displacement for Vehicle II, the maximum brake effective pressure is maintained within 10% variation at most so that the scaled engine can be practical. The minimal energy consumption of Vehicle I and II is evaluated through both FACE and VHOT.

Results and Analysis

The minimum energy consumption of Vehicle I and II is illustrated and compared in Fig. 6.6 over NEDC and HYWFET. Concerning Vehicle I, the minimum energy consumption approximated by FACE is the same as the one evaluated through QSS in terms of VHOT. This is due to the application of the same type powertrain model. As for Vehicle II,

Vehicle		I	II
	m_v [kg]	1814	
	R_w [m]	0.3173	
	C_{v0} [N]	93.5	
	C_{v1} [N/(m/s)]	5.29	
	C_{v2} [N/(m/s)^2]	0.536	
Engine	$\mathcal{I}_e$	SI/NA/SB	
	$\mathcal{V}_e$ [L]	1.40	1.26
	$\mathcal{T}_e$ [Nm]	130	
	$\mathcal{P}_e$ [kW]	60	
Battery	$\mathcal{I}_b$	HP	
	$\mathcal{Q}_b$ [Ah]	31	
	$\mathcal{K}_b$	54	
Electric Motor	$\mathcal{I}_m$	PMSM	
	$\mathcal{T}_m$ [Nm]	28	
	$\mathcal{P}_m$ [kW]	37	
Drivetrain	$\mathcal{I}_t$	MT-5	

Table 6.2 – Main features of investigated parallel hybrid-electric vehicles.

the minimal energy consumption of FACE is slightly higher than the one of VHOT. However, the differences is neglected due to its small magnitude.

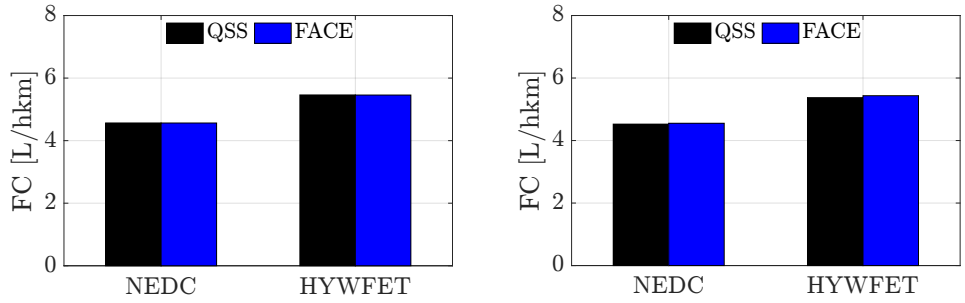

(a) Vehicle I

(b) Vehicle II

Figure 6.6 – Minimal energy consumption of reference and investigated parallel hybrid electric vehicles.